Stratigraphic Modeling: A Step Beyond AVO

Yinbin Liu*, Geophysical Researcher, Calgary, AB, Canada
yinbin@telus.net

ABSTRACT

Stratigraphic modeling studies seismic reflection characterizations within sedimentary sequences to provide clues for stratigraphic and reservoir interpretations. This work models scale-dependent multiple scattering of waves within sedimentary sequences for both normal and oblique incidences. The interference of multiple waves results in low frequency behavior for the primary arrivals and high frequency coda waves for the tail. The coda waves are composed of P-coda and SV-coda waves. The P-coda waves play a dominant rule in small incidence angle or near offset and vice versa the SV-coda waves for large incidence angle or far offset. This property of multiple scattering of waves within sedimentary sequence is similar with that of reflection coefficient of a single interface for AVO analysis. The result suggests that coda waves caused by the multiple scattering of waves within sedimentary sequence are probably useful clues for finding stratigraphic traps from seismic data.

Introduction

Seismic modeling simulates seismic response for an assumed geological geometry. There are different scale modelings for exploration geophysics. For example, structural modeling (large-scale) relates to identifications of structural traps; stratigraphic modeling (small-scale) relates identifications of lithologic changes and stratigraphic traps; and reservoir modeling (macro-scale) relates to the simulation of fluid content. This work mainly discuss multiple reflection characterizations within sedimentary sequences to provide clues for stratigraphyic (or lithologic change) and reservoir interpretations.

Seismic wave scattering is strongly dependent on the inhomogeneous scale of medium. Ray theory (Snell's law) best describes wave propagation when the scale of heterogeneity is larger than seismic wavelength (high frequency or short-wavelength approximation). Effective medium theory (e.g., Backus, 1962) describes wave propagation when the scale of heterogeneity is much less than seismic wavelength (low frequency or long-wavelength approximation). For intermediate frequencies, where the scale of heterogeneity is comparable to seismic wavelength, multiple scattering of waves may have singnificant influence on waveform distortion.

A universal feature of sedimentary sequences is that they tend to be layered. Reservoir thicknesses within these sequences are usually much less than seismic wavelengths. A single sedimentary layer is usually hard to be detected and captured by surface seismic.

However, the over-all change in pore fluid and stratigraphy (or lithology change) within depositonal sequences may have singnificant influence on signal distortion because of multiple scattering of waves, especially for the depositional sequence with strong impedance contrasts like as macro-layers of gas sand and coal interbedded with shale. A strong reflection on seismic data may not be to come from large impedance contrast but the constructive interference of multiple scattering waves (Lindseth, 1979). On the other hand, there are also seismically 'dim' reservoirs because of the destructive interference of multiple scattering waves.

Seismic amplitude variation with offset (AVO) is a major criterion for identification of gas. However, sometimes it does not work well because of the oversimplified geological geometry assumption for AVO analysis. AVO modeling based on the reflection of a single interface does not explain volume scattering within sedimentary sequences. The multiple scattering of waves within sedimentary sequences carries the information on lithological changes and may be used to extract stratigraphic traps from seismic data.

Model and algorithm

We consider plane wave propagation through a quasiperiodic limestone/shale stack embedded between two shale half-spaces. For convenience, the influence of shear waves in two shale half-space is ignored. The shale and limestone have the same thickness $d_1 = d_2$ with the spatial period $d = d_1 + d_2$ and a periodic structure of 'M'. M=1 denotes limestone/shale (two layers) and M=2 denotes limestone/shale/ limestone/shale (four layers), et. al.. The properties of the constituent materials are given in Table 1. The corresponding Thomson's anisotropic parameters (Thomson, 1986) are shown in Table II. The intrinsic anisotropy of shale (Wang, 2002) does not be considered in this work.

The changing scale models ($R = \lambda / d$, where λ is the seismic wavelength of transmission signal) are constructed by choosing a different spatial periodic 'M' (or arrangement) and keeping the total thickness ('D') = M*d and the proportion of materials (Marion et al., 1994, Liu and Schmitt, 2002). The individual layers change thickness from near seismic wavelength (small M, ray theory) to much less than seismic wavelength (large M, effective medium theory). A propagation matrix method is employed to study the multiple scattering in limestone/shale stacks. The incident plane wave is a single cycle pulse with a 50hz dominant frequency.

Table I. Parameters of constituent materials

Medium	$v_c (m/s)$	$v_s (m/s)$	$\rho (g/cm^3)$
limestone	5540	3040	2.7
shale	2743	1509	2.38

Table II. Thomsen anisotropic parameters

Medium	α_0 (m/s)	β_0 (m/s)	ε	δ	γ	ρ (g/cm^3)
limestone /shale	3405	1872	0.3	0.001	0.35	2.54

Numerical results

For exploration geophysics, seismic velcoity information is used to imagie geological structures (large-scale) and seismic amplitude and waveform information is used to identify small-scale stratigraphy and reservoirs (Rummerfield, 1954; O'Doherty and Ansty, 1971; Neidell and Poggiagliomi, 1977). Seismic reflection waveform variation with offset or angle for layered system has important implications for identifying lithology, stratigraphy, and pore fluid content.

For limestone/shale stack, the critical angles based on ray theory are $\theta_c = 29.7^0$ for P-wave and $\theta_s = 64.5^0$ for SV-wave; and the P-wave critical angle based on effective medium theory is $\theta_{ec} = 42.8^0$ (no SV-wave critical angle). Figures 1 and 2 show the calculated transmission (Figures 1a, 1b, and 1c) and reflection (Figures 2a, 2b, and 2c) waveforms for the stacks of limestone/shale layers with a total thickness of 400m and same individual layer thickness for different incident angles. The thickness of the individual layers change from d_1 = d_2 = 200m for M=1 (ray theory) to d_1 = d_2 = 0.78m for M = 256 (effective medium theory). Figures 1a and 2a are normal incidence and Figures 1b and 2b are moderate angle incidence ($\theta = 20^0 < \theta_c$) and Figures 1c and 2c are large angle incidence ($\theta_c < \theta = 35^0 < \theta_{ec}$). The value $R = \lambda/d$ are also shown in the Figures 1a and 2a for normal incidence (from R = 0.2 to 50). The R values for oblique incidence do not be given out because the travel pathes for oblique incidence are not straight lines.

Multiple scattering of waves Figures 1a to 2c show that multiple scattering results in velocity dispersion and waveform distortion. Velocity dispersion is because the direct wave is rapidly reduced to negligible value and the multiple waves become the first arrivals. Waveform distortion occurs as low frequency behavior and coda waves (P-coda and SV-coda waves). The low frequency wave is due to the buildup of the interference of multiple reflections. Amplitude and frequency of the wave increase, whereas duration time decreases with decreasing inhomogeneous scale or increasing R. The low frequency wave occurs as either coherent scattering attenuation for small R, which is due to the destructive interference of the multiple scattering, or coherent scattering enhancement for large R, which is due to the constructive interference of the multiple scattering. As R increases further, the low-frequency energy transfers into an enhanced main wave type and high frequency coda waves. The amplitude and frequency of the coda waves decrease and increase, respectively, with increasing R. In the effective medium region, the energies of the coda waves decreases to zero and all of the energies transfers into a direct transmission wave (Figure 1) and reflection wave (Figure 2) in a transversely isotropic effective medium (Liu and Schmitt, 2002). The transmission wave is strong and the reflection wave is weak in effective medium region. The velocity dispersion is obvious for the first arrived transmission waves (Figure 1) but there is no velocity dispersion for the first arrived reflection waves (Figure 2). This shows that the reflection on the first individual layer has dominant influence on the arrival time of reflection waves. It can also be seen that waveform distortions take place at a wider range (between R =0.7 and 25).

Small and moderate angle reflections The waveform transitions from ray to effective medium theories for normal and moderate angle ($\theta = 20^0 < \theta_c = 29.7^0$) incidences are shown in Figure 1a and 1b for transmissions and 2a and 2b for reflections. The pulses following the direct P-wave are multiple P-wave for M=1 and M=2 in Figures 1a and 2a but the direct SV-wave for M=1 in Figure 1b (or the multiple reflection P-wave in Figure 2b). For larger M, the interference of multiple scattering waves results in P-coda waves in Figures 1a and 2a (no shear wave) and P-coda and SV-coda waves for Figures 2a and 2b. The coda waves in Figures 1b and 2b are a little more complex than those of normal incidence because of the influence of SV-wave for oblique incidence. The P-coda wave (or scattering P-wave) and SV-coda wave (or scattering SV-wave) will convert each other during propagation. The superposition of the multiple scattering waves may cause destructive interference (scattering attenuation) and constructive interference (scattering enhancement). The strength of the P-coda and SV-coda waves is dependent on heterogeneous scale, impedance contrasts, and incident angle. In effective medium region, the transmission waves transfer into qP-wave and qSV-wave in a transversely isotropic medium. The qSV-wave in Figure 1b has much less amplitude than that of qP-wave but can be clearly seen at M = 96, 128, and 256.

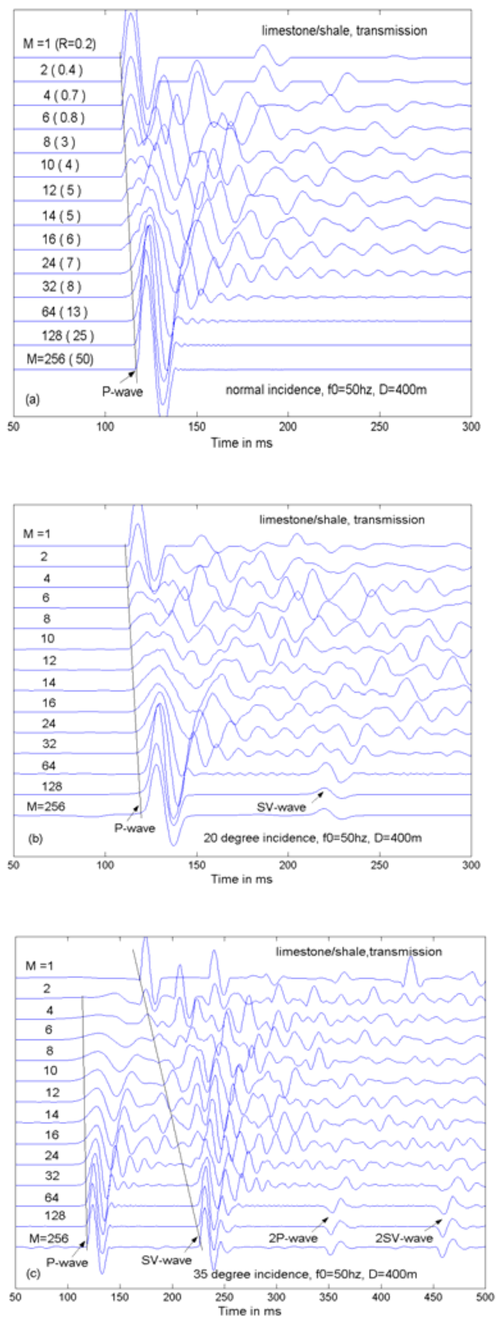

Figure 1: Theoretical transmission waveforms for limestone/shale stack with M =1 to 256 and a total thickness of 400m. The incident plane wave is a single cycle pulse with a 50hz dominant frequency. (a) normal incidence; (b) 20 degree incidence; and (c) 35 degree incidence.

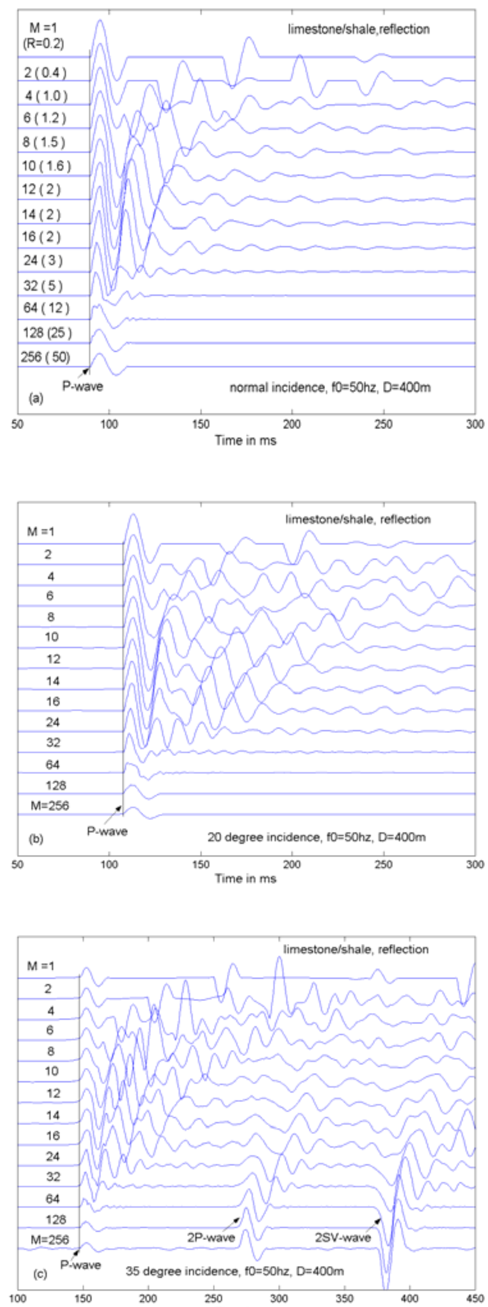

Figure 2: Theoretical reflection waveforms for limestone/shale stack with M =1 to 256 and a total thickness of 400m. The incident plane wave is a single cycle pulse with a 50hz dominant frequency. (a) normal incidence; (b) 20 degree incidence; and (c) 35 degree incidence.

Large angle reflection The waveform transitions from ray to effective medium theories for large angle incidence ($\theta_c < \theta = 35^0 < \theta_{ec}$) are shown in Figure 1c for transmissions and Figure 2c for reflections. It can be seen from Figure 1c that the first arrivals are SV-wave for small M (M=1) but scattering P-wave for large M. The types of the first arrivals will transfer from SV-wave to scattering waves (scattering P-wave, scattering SV-wave, and converted scattering wave) and to the qP-wave in an equivalent transversely isotropic medium. There are no clear transition boundaries from ray region to scattering region to effective medium region. The coda waves following P-wave are mainly P-coda waves and the coda waves following SV-wave are mainly SV-coda waves in Figure 1c. The energies of the SV-wave and SV-coda waves are stronger than those of the P-coda and P-coda waves because scattering SV-wave plays a dominant role in large angle incidence. The coda waves following P-wave in Figure 2c are mainly SV-coda waves, which has stronger energy than the reflection P-wave. This indicates that SV-coda waves will play a dominant role for large angle reflections, which is similar with that of reflection coefficient of a single interface for AVO analysis. The multiple qP-wave (2P-wave) and qSV-wave (2SV-wave) from the top and bottom interfaces are also shown in Figures 1c and 2c. The energy of the multiple qSV-wave is stronger than that of multiple qP-wave for large angle incidence.

Conclusions and discussions

The multiple scattering of seismic waves within sedimentary sequence causes low frequency behavior and coda waves, which are strongly dependent on heterogeneous scale, impedance contrast, and incident angle. The P-coda waves play a dominant rule in small incidence angle or near offset and vice versa the SV-coda waves for large incidence angle or far offset. Forward modeling based on well log data (the borehole scale, tens of centimeters) makes it possible to match actual surface seismic data (the surface scale, tens of meters). It is beneficial to choose representative records at each area and establish standard seismic responses so as to provide a common basis for stratigraphic (or lithologic) and reservoir interpretation. The multiple scattering of seismic waves within sedimentary sequence provides a useful clue to resolve small-scale stratigraphy and lithology.

References

Backus, G. E., 1962, Long-wave elastic anisotropy produced by horizontal layering: J. Geophys. Res., 67, 4427-4440.

Marion, D. P., Mukerji, T. and Mavko, G., 1994, Scale effects on velocity dispersion: From ray to effective medium theories in stratified media: Geophysics, 59,1613-1619.

Stratigraphic modeling

Lindseth, R. O., 1979, Synthetic sonic logs - a process for stratigraphic interpretation: Geophysics, 44, 3-26.

Liu, Y., and Schmitt, D. R., 2002, Seismic scale effects: dispersion, attenuation, and anisotropy by multiple scattering of waves, Ann. Mtg., Canadian Soc. Expl. Geophys., Expanded Abstracts.

Neidell, N. S. and Poggiagliomi, E., 1977, Stratigraphic modeling and interprtation: Geophysical principles and techniques, in AAPG memoir 26, Seismic Stratigraphy – Application to Hydrocarbon Exploration, Eds, Charles E. Payton, 389-416.

O'Doherty R. F. and Anstey N. A., 1971, Reflections on amplitudes: Geophys. Pros., 19, 430-458.

Rummerfield, N. F., 1954, Reflection quality, A fourth dimension, Geophysics, 29, 684-694.

Thomsen, L., 1986, Weak elastic anisotropy, Geophysics, 51, 1954-1966.

Wang, Z., 2002, Seismic anisotropy in sedimentary rocks, part 2: Laboratory data, Geophysics, 67,1423-1440.